



---

*Research article*

## Dynamics of a predator-prey model with fear effects and gestation delays

Yaping Wang, Yuanfu Shao\* and Chuanfu Chai

College of Science, Guilin University of Technology, Guilin, Guangxi 541004, China

\* **Correspondence:** Email: shaoyuanfu@163.com; Tel: +8615877039525.

**Abstract:** Recent studies have shown that, in addition to direct predation, fear of predators alters the physiological behavior of prey. Based on this fact, this paper investigates a three-species food chain based on ratio-dependent and Beddington-DeAngelis type functional responses, which incorporates fear effects and two gestation delays. The positivity, boundedness and existence of equilibrium points of the system are investigated, and the local stability behavior of the equilibrium points and the occurrence of Hopf-bifurcation when the time lag parameters exceed the critical values are studied by analyzing the corresponding characteristic equations. The main results show that Hopf-bifurcation occurs when the time delay parameters attain the thresholds. Finally, numerical simulations are performed to verify our main results.

**Keywords:** food chain model; fear effect; delays; stability analysis; Hopf-bifurcation

**Mathematics Subject Classification:** 34C23, 92D25

---

### 1. Introduction

Predator-prey interactions play an important role in shaping community structure and maintaining ecological diversity. Over the past few decades, food chain models have been extensively studied and a large number of papers have been published. Researchers have used mathematical models to understand the complexity of ecosystems and predict the consequences of ecosystems [1–8].

Generally, predators affect prey populations by killing them directly, but many recent studies [9–11] have shown that fear effects play a crucial role in ecology and evolutionary biology. In [9], fear was found to cause prey species to exhibit many anti-predator behaviors and defense mechanisms. In [10], prey birth and death rates were affected by fear of predation risk. In [11], higher levels of fear were found to result in lower equilibrium levels of coexistence and global asymptotic stability of species near equilibrium. Their results all point to the importance of fear in predator-prey systems. The presence of predators forces prey to be more alert and spend less time foraging or choosing new habitats due to the fear of being killed, while fear also reduces the mating rate of prey populations, resulting in a

decrease in prey population size. In 2011, Zanette et al. [12] used song sparrows as subjects for their experiments. They left the population of song sparrows in a predator-free area and then manipulated artificial predation risk by playing the sounds of predators. Through experiments, they observed that the song sparrows' perception of predation risk led to a reduction in their breeding population by about 40% compared to the previous population. So this experiment confirms that fear reduces the reproductive rate of prey. In another experiment involving elk, Creel et al. [13] observed that the risk of predation by wolves caused elk to remain alert and move to areas with low predation risk. This suggests that the physiological behavior of elk is influenced by anti-predator behavior. Suraci et al. [14] used sound playback of large carnivores to induce fear in medium carnivores and found that fear of large carnivores increased vigilance and greatly reduced foraging behavior in medium carnivores. These experiments all confirm the important effects of fear on the dynamic behavior of species. In recent years, many researchers have proposed that the predator-prey system should incorporate a fear factor. In 2016, Wang et al. [15] proposed a mathematical model with fear and confirmed the importance of fear on the growth of prey.

In ecology, how predators feed on prey is a very important factor, and the way they interact with each other affects the dynamics of the entire ecosystem. This interaction is called the “functional response”, which gives the per capita rate of the predator feeding on prey and is a key component of the mathematical model, allowing us to study the dynamics of the model in a better way. The most widely used functional responses include Holling type II, Holling type III, Holling type IV [16–18], Monod-Haldane functional response, Beddington-DeAngelis functional response, Crowley-Martin functional response and the ratio-dependent functional responses, etc. [19–23]. The Holling type II functional response is the more commonly used functional response, but this functional response depends only on prey density and is not applicable for ecosystems with large population sizes. To achieve the elimination of this situation, we introduce a ratio-dependent functional response, which is determined simultaneously by the relationship between prey density and predator density. In particular, when predators have to go in search of food, they will face a situation of sharing and competition with other predators. Therefore, ratio-dependent functional responses will be more closely related to practicality. Also, considering that predators are disturbed by other predators while handling or searching for prey, the Beddington-DeAngelis functional response deserves further study. Therefore, we will consider introducing ratio-dependent functional response and Beddington-DeAngelis functional response in the model.

Delay differential equations (DDEs) have a long history in modeling predator-prey systems, where delays usually represent the required reaction time, gestation period, maturation, feeding time, etc. [24–29]. In terms of mathematical modeling, delayed systems [30, 31] make more sense than non-delayed systems. The introduction of time delays in a predator-prey model causes the model to exhibit more complex dynamics. Among them, the gestation delay represents the time delay that occurs when biomass is transferred from prey to predator. For example, Tripathy et al. [5] investigated the degree of mutual interference between density-dependent predators in a model incorporating discrete gestation delays and Beddington-DeAngelis-type functional responses. They observed that when the delay parameter exceeded a certain threshold, the system experienced Hopf bifurcation and the system lost its stability. Based on this finding, they investigated two different time delay effects in a proportionally dependent predator-prey system and studied the conditions under which Hopf-bifurcation occurred when both delays were present in the model. From the above example, we can

determine the importance of delay in stability analysis. Therefore, we add the time lag parameters to the model.

In this paper, we aim to study the effect of time lag parameters on the dynamics of the system. The rest of the paper is organized as follows. In the next section, we construct a predator-prey model with fear effects and multiple delays. In Section 3, we analyze the positivity and boundedness of the solutions of the system. In Section 4, we present the criterion of the existence of equilibrium points. In Section 5, we study the stability of the equilibrium point and the conditions of the occurrence of Hopf bifurcation with time lags as the bifurcation parameter. In Section 6, we use numerical simulations to verify our main analytical results. Finally, we conclude the whole paper.

## 2. Model formulation

Let  $x_1(t)$ ,  $x_2(t)$ , and  $x_3(t)$  be the population densities of prey, intermediate predator, and top predator at time  $t$ , respectively. We construct the mathematical model through the following assumptions.

(1) In the absence of predators, the prey population increases logically. However, in the presence of intermediate predators, the prey perceives fear, and fear affects the reproductive rate of the prey.

(2) Intermediate predators prey on preys based on a ratio-dependent functional response. However, the interaction between intermediate and top predators follows a Beddington-DeAngelis type functional response. Among them, the expression form of the ratio-dependent functional response is  $f(x_1, x_2) = \frac{\alpha x_1}{x_1 + mx_2}$ , and the expression form of the Beddington-DeAngelis type functional response is  $f(x_2, x_3) = \frac{\theta x_2}{v + px_2 + qx_3}$ .

(3) Most biological processes involve delays, and here we consider two gestation delays, a time interval between the predator preying on its prey and the prey breeding offspring, denoted by  $\tau_1, \tau_2$ .

Based on these assumptions, we obtain the following model:

$$\begin{aligned} \frac{dx_1}{dt} &= \frac{rx_1}{1 + kx_2} - bx_1 - ax_1^2 - \frac{\alpha x_1 x_2}{x_1 + mx_2}, \\ \frac{dx_2}{dt} &= \frac{\beta x_1(t - \tau_1)x_2(t - \tau_1)}{x_1(t - \tau_1) + mx_2(t - \tau_1)} - dx_2 - \frac{\theta x_2 x_3}{v + px_2 + qx_3}, \\ \frac{dx_3}{dt} &= \frac{\eta x_2(t - \tau_2)x_3(t - \tau_2)}{v + px_2(t - \tau_2) + qx_3(t - \tau_2)} - ex_3, \end{aligned} \quad (2.1)$$

where  $r, k, b, a$  and  $\alpha$  are the intrinsic growth rate of prey, intermediate predator-induced fear, mortality, intraspecific competition rate and prey consumption rate, respectively. Meanwhile,  $\beta, d, \theta, \eta$  and  $e$  are prey conversion rate, intermediate predator mortality and consumption rate, intermediate predator conversion rate and top predator mortality rate, respectively. Here  $m$  is the half-saturation constant of the ratio-dependent functional response,  $v$  is the saturation constant of the Beddington-DeAngelis-type functional response.  $p$  and  $q$  are the abundance of intermediate predators and disturbance of top predators, respectively.  $\tau_1$  and  $\tau_2$  represent gestation time delays.

The initial conditions are

$$x_1(s) = \phi_1(s), \quad x_2(s) = \phi_2(s), \quad x_3(s) = \phi_3(s), \quad -\tau \leq s \leq 0, \quad (2.2)$$

where  $\tau = \max\{\tau_1, \tau_2\}$ ,  $\Phi = (\phi_1, \phi_2, \phi_3)$ , and  $\Phi = (\phi_1, \phi_2, \phi_3)$  belongs to the Banach space of

continuous function  $\Phi : [-\tau, 0] \rightarrow R^3$  with

$$\|\Phi\| = \sup_{-\tau \leq s \leq 0} (|\phi_1(s)|, |\phi_2(s)|, |\phi_3(s)|).$$

From the biological perspective, we assume  $\phi_i(s) \geq 0$  and  $\phi_i(0) > 0$ ,  $i = 1, 2, 3$ .

### 3. Positivity and boundedness of solutions

**Theorem 3.1.** *All solutions of system (2.1) with initial conditions (2.2) are positive for all  $t > 0$ .*

*Proof.* System (2.1) can be written in the following matrix form:

$$\dot{W} = F(W),$$

$$\text{where } W = \begin{pmatrix} x_1 \\ x_2 \\ x_3 \end{pmatrix}, \text{ and } F(W) = \begin{pmatrix} F_1(W) \\ F_2(W) \\ F_3(W) \end{pmatrix} = \begin{pmatrix} \frac{rx_1}{1+kx_2} - bx_1 - ax_1^2 - \frac{\alpha x_1 x_2}{x_1 + mx_2} \\ \frac{\beta x_1(t-\tau_1)x_2(t-\tau_1)}{x_1(t-\tau_1)+mx_2(t-\tau_1)} - dx_2 - \frac{\theta x_2 x_3}{v+px_2+qx_3} \\ \frac{\eta x_2(t-\tau_2)x_3(t-\tau_2)}{v+px_2(t-\tau_2)+qx_3(t-\tau_2)} - ex_3 \end{pmatrix} \text{ with the initial condition}$$

$$W(s) = (\phi_1(s), \phi_2(s), \phi_3(s)) \in C[-\tau, 0], R_+^3 \text{ and } \phi_1(0), \phi_2(0), \phi_3(0) > 0.$$

We have easily checked in system (2.1) that whenever choosing  $W(s) \in R_+^3$ , then

$$F_i(W)|_{W \in R_+^3} \geq 0, \quad i = 1, 2, 3.$$

Using the Lemma 4 given in [32], we obtain that every solution  $W(t)$  of the system (2.1) with initial conditions (2.2) exists in the region  $R_+^3$  and is positive and invariant for all  $t > 0$ .  $\square$

**Theorem 3.2.** *The solutions of system (2.1) which starts in  $R_+^3$  are uniformly bounded.*

*Proof.* Let  $U(t) = x_1(t - \tau_1 - \tau_2) + \frac{\alpha}{\beta}x_2(t - \tau_2) + \frac{\alpha\theta}{\beta\eta}x_3(t)$ .

Calculating the derivative of  $U(t)$  along the solution of system (2.1), we have

$$\begin{aligned} \frac{dU}{dt} &= \frac{dx_1}{dt}(t - \tau_1 - \tau_2) + \frac{\alpha}{\beta} \frac{dx_2}{dt}(t - \tau_2) + \frac{\alpha\theta}{\beta\eta} \frac{dx_3}{dt}(t) \\ &= \frac{rx_1(t - \tau_1 - \tau_2)}{1 + kx_2(t - \tau_1 - \tau_2)} - bx_1(t - \tau_1 - \tau_2) - ax_1^2(t - \tau_1 - \tau_2) - \frac{\alpha x_1(t - \tau_1 - \tau_2)x_2(t - \tau_1 - \tau_2)}{x_1(t - \tau_1 - \tau_2) + mx_2(t - \tau_1 - \tau_2)} \\ &\quad + \frac{\alpha x_1(t - \tau_1 - \tau_2)x_2(t - \tau_1 - \tau_2)}{x_1(t - \tau_1 - \tau_2) + mx_2(t - \tau_1 - \tau_2)} - \frac{\alpha d}{\beta} x_2(t - \tau_2) - \frac{\alpha\theta}{\beta} \frac{x_2(t - \tau_2)x_3(t - \tau_2)}{v + px_2(t - \tau_2) + qx_3(t - \tau_2)} \\ &\quad + \frac{\alpha d}{\beta} x_2(t - \tau_2) - \frac{\alpha\theta}{\beta} \frac{x_2(t - \tau_2)x_3(t - \tau_2)}{v + px_2(t - \tau_2) + qx_3(t - \tau_2)} - \frac{\alpha\theta e}{\beta\eta} x_3(t) \\ &\leq rx_1(t - \tau_1 - \tau_2) - bx_1(t - \tau_1 - \tau_2) - ax_1^2(t - \tau_1 - \tau_2) - \frac{\alpha d}{\beta} x_2(t - \tau_2) - \frac{\alpha\theta e}{\beta\eta} x_3(t) \\ &\leq \frac{r^2}{4a} - \min\{b, d, e\} U(t). \end{aligned}$$

Let  $z = \min\{b, d, e\}$  and  $Q = \frac{r^2}{4a}$ . Using the theory of differential inequality [33], we obtain

$$0 < U(t) \leq \frac{Q}{z} (1 - e^{-zt}) + U(0)e^{-zt}.$$

When  $t \rightarrow \infty$ , we get  $0 < U \leq \frac{Q}{z}$ . Therefore, all the solutions of system (2.1) starting from  $R_+^3$  are restricted in the region:

$$D = \left\{ (x_1, x_2, x_3) \in R_+^3 : 0 < U \leq \frac{Q}{z} \right\}.$$

This completes the proof.  $\square$

#### 4. Equilibrium points and their criteria of existence

The possible equilibrium points of the model are as follows:

(1) The trivial equilibrium point  $E_0(0, 0, 0)$  always exists.

(2) The predator free axial equilibrium point  $E_1\left(\frac{r-b}{a}, 0, 0\right)$  exists if  $r > b$ .

(3) The top predator free equilibrium point  $E_2(\bar{x}_1, \bar{x}_2, 0)$  where  $\bar{x}_2 = \frac{\beta-d}{md}\bar{x}_1$  and  $\bar{x}_1$  is a positive root of  $-ac(1+cm)x_1^2 - [(1+cm)(cb+a) + c^2\alpha]x_1 + (r-b)(1+cm) - c\alpha = 0$ , where  $c = \frac{\beta-d}{md}$ . According to Descartes's rule of sign, the equation must have a unique positive root if  $(r-b)(1+cm) > c\alpha$ . Thus, the equilibrium  $E_2$  exists if  $(r-b)(1+cm) > c\alpha$ .

(4) The interior equilibrium point  $E^*(x_1^*, x_2^*, x_3^*)$  exists if the following two isoclines have a positive intersection:

$$\begin{cases} f(x_1, x_2) = A_1x_1^2 + B_1x_1 + C_1 = 0, \\ g(x_1, x_2) = A_2x_2^2 + B_2x_2 + C_2 = 0, \end{cases}$$

where

$$\begin{aligned} x_3^* &= \rho_1x_2^* - \rho_2, \quad \rho_1 = \frac{\eta - pe}{qe}, \quad \rho_2 = \frac{v}{q}, \\ A_1 &= -a(1 + kx_2) < 0, \\ B_1 &= r - (1 + kx_2)(b + amx_2), \\ C_1 &= x_2[rm - (mb + \alpha)(1 + kx_2)], \\ A_2 &= -m[d(p + \rho_1q) + \theta\rho_1] < 0, \\ B_2 &= \beta x_1(p + \rho_1q) + d[(p + \rho_1q)x_1 + mv - \rho_2mq] - \theta(\rho_2x_1 - m), \\ C_2 &= \beta x_1(v - \rho_2q) - dx_1(v - \rho_2q) + \rho_2\theta x_1. \end{aligned}$$

As  $x_2 \rightarrow 0$ , then the above two isoclines become:

$$\begin{cases} f(x_1, 0) = -ax_1^2 + (r-b)x_1 = 0, \\ g(x_1, 0) = C_2 = 0, \end{cases}$$

where the number of positive roots of the  $f(x_1, 0) = 0$  depends on the sign of  $r - b$ , then the above two isoclines have a unique intersection on the first quadrant (the positive quadrant) if the following sufficient condition holds:

$$\begin{cases} r > b, \\ \frac{dx_2}{dx_1} = -\frac{\partial f(x_1, x_2)/\partial x_1}{\partial f(x_1, x_2)/\partial x_2} < 0, \\ \frac{dx_2}{dx_1} = -\frac{\partial g(x_1, x_2)/\partial x_1}{\partial g(x_1, x_2)/\partial x_2} > 0. \end{cases}$$

## 5. Local stability and Hopf bifurcation

In this section, our goal is to determine the local behavior of the system (2.1) around the equilibrium point. First, system (2.1) can be expressed as

$$\frac{dW}{dt} = F(W(t), W(t - \tau_1), W(t - \tau_2)),$$

where  $W(t) = [x_1(t), x_2(t), x_3(t)]^T$ .

We take  $E(x_1, x_2, x_3)$  as an arbitrary equilibrium point of the system (2.1). Assume  $\tilde{x}_1(t) = x_1(t) - x_1$ ,  $\tilde{x}_2(t) = x_2(t) - x_2$  and  $\tilde{x}_3(t) = x_3(t) - x_3$ . Then, the linearized system (2.1) around the equilibrium point  $E$  is

$$\frac{dG}{dt} = D_1 G(t) + D_2 G(t - \tau_1) + D_3 G(t - \tau_2),$$

where

$$D_1 = \left( \frac{\partial F}{\partial W(t)} \right)_E, \quad D_2 = \left( \frac{\partial F}{\partial W(t - \tau_1)} \right)_E, \quad D_3 = \left( \frac{\partial F}{\partial W(t - \tau_2)} \right)_E,$$

and  $G(t) = [\tilde{x}_1(t), \tilde{x}_2(t), \tilde{x}_3(t)]^T$ . The Jacobian matrix of the system (2.1) at  $E$  is given by

$$J = D_1 + D_2 e^{-\lambda\tau_1} + D_3 e^{-\lambda\tau_2}.$$

Then

$$J = \begin{bmatrix} a_{11} & a_{12} & 0 \\ b_{21} e^{-\lambda\tau_1} & a_{22} + b_{22} e^{-\lambda\tau_1} & a_{23} \\ 0 & c_{32} e^{-\lambda\tau_2} & a_{33} + c_{33} e^{-\lambda\tau_2} \end{bmatrix},$$

where

$$\begin{aligned} a_{11} &= \frac{r}{1 + kx_2} - b - 2ax_1 - \frac{\alpha mx_2^2}{(x_1 + mx_2)^2}, & a_{12} &= -\frac{krx_1}{(1 + kx_2)^2} - \frac{\alpha x_1^2}{(x_1 + mx_2)^2}, \\ a_{22} &= -d - \frac{\theta x_3(v + qx_3)}{(v + px_2 + qx_3)^2}, & a_{23} &= -\frac{\theta x_2(v + px_2)}{(v + px_2 + qx_3)^2}, & a_{33} &= -e, \\ b_{21} &= \frac{\beta mx_2^2}{(x_1 + mx_2)^2}, & b_{22} &= \frac{\beta x_1^2}{(x_1 + mx_2)^2}, & c_{32} &= \frac{\eta x_3(v + qx_3)}{(v + px_2 + qx_3)^2}, & c_{33} &= \frac{\eta x_2(v + px_2)}{(v + px_2 + qx_3)^2}. \end{aligned}$$

According to the Jacobian matrix, we analyze the stability of the equilibrium point  $E_0$ ,  $E_1$  and  $E_2$ , and obtain the following theorems:

**Theorem 5.1.** *The trivial equilibrium point  $E_0(0, 0, 0)$  is locally asymptotically stable if  $r < b$  and becomes unstable if  $r > b$ .*

**Theorem 5.2.** *When  $\tau_1 \geq 0$ , the predator free axial equilibrium point  $E_1\left(\frac{r-b}{a}, 0, 0\right)$  is locally asymptotically stable if  $\beta < d$ ; otherwise it is unstable.*

**Theorem 5.3.** *For system (2.1), according to the value of  $\tau_1$ , there are the following two cases:*

- (1) *When  $\tau_1 = 0$ , the top predator free equilibrium point  $E_2 = (\bar{x}_1, \bar{x}_2, 0)$  is locally asymptotically stable for any  $\tau_2 \geq 0$  if  $\bar{x}_2 < \frac{ve}{\eta - pe}$ ,  $a\bar{x}_1 + d + \frac{\beta\bar{x}_1^2}{(\bar{x}_1 + m\bar{x}_2)^2} > \frac{\alpha\bar{x}_1\bar{x}_2}{(\bar{x}_1 + m\bar{x}_2)^2}$  and  $\left(-a\bar{x}_1 + \frac{\alpha\bar{x}_1\bar{x}_2}{(\bar{x}_1 + m\bar{x}_2)^2}\right)\left(\frac{\beta\bar{x}_1^2}{(\bar{x}_1 + m\bar{x}_2)^2} - d\right) + \frac{\beta m\bar{x}_2^2}{(\bar{x}_1 + m\bar{x}_2)^2} \left(\frac{kr\bar{x}_1}{(1 + k\bar{x}_2)^2} + \frac{\alpha\bar{x}_1^2}{(\bar{x}_1 + m\bar{x}_2)^2}\right) > 0$ ; otherwise unstable.*

(2) When  $\tau_1 > 0$  and  $\bar{x}_2 < \frac{ve}{\eta-pe}$ , if  $H_2^2 - N_2^2 < 0$  and  $2\varphi_0^2 + H_1 - N_1^2 - 2H_2 > 0$  hold, the super predator free equilibrium point  $E_2 = (\bar{x}_1, \bar{x}_2, 0)$  is locally asymptotically stable for  $\tau_1 \in [0, \hat{\tau}_1)$  and unstable for  $\tau_1 > \hat{\tau}_1$ . Moreover, the system (2.1) undergoes a Hopf bifurcation when  $\tau_1 = \hat{\tau}_1$ , where

$$\hat{\tau}_1 = \min_{j=0,1,2,\dots} \tau_{1j} = \min_{j=0,1,2,\dots} \left[ \frac{1}{\varphi_0} \arccos \left[ \frac{N_2(\varphi_0^2 - H_2) - H_1 N_1 \varphi_0^2}{N_1^2 \varphi_0^2 + N_2^2} \right] + \frac{2\pi j}{\varphi_0} \right],$$

and  $\varphi_0$  is defined in the proof.

Next, we study the local stability of  $E^* = (x_1^*, x_2^*, x_3^*)$ . The Jacobian matrix at  $E^*$  is

$$J_{E^*} = \begin{bmatrix} A_{11} & A_{12} & 0 \\ B_{21}e^{-\lambda\tau_1} & A_{22} + B_{22}e^{-\lambda\tau_1} & A_{23} \\ 0 & C_{32}e^{-\lambda\tau_2} & A_{33} + C_{33}e^{-\lambda\tau_2} \end{bmatrix},$$

where

$$\begin{aligned} A_{11} &= -ax_1^* + \frac{\alpha x_1^* x_2^*}{(x_1^* + mx_2^*)^2}, & A_{12} &= -\frac{krx_1^*}{(1 + kx_2^*)^2} - \frac{\alpha(x_1^*)^2}{(x_1^* + mx_2^*)^2}, \\ A_{22} &= -d - \frac{\theta x_3^*(v + qx_3^*)}{(v + px_2^* + qx_3^*)^2}, & A_{23} &= -\frac{\theta x_2^*(v + px_2^*)}{(v + px_2^* + qx_3^*)^2}, \\ A_{33} &= -e, & B_{21} &= \frac{\beta m(x_2^*)^2}{(x_1^* + mx_2^*)^2}, & B_{22} &= \frac{\beta(x_1^*)^2}{(x_1^* + mx_2^*)^2}, \\ C_{32} &= \frac{\eta x_3^*(v + qx_3^*)}{(v + px_2^* + qx_3^*)^2}, & C_{33} &= \frac{\eta x_2^*(v + px_2^*)}{(v + px_2^* + qx_3^*)^2}. \end{aligned}$$

The corresponding characteristic equation of the above Jacobian matrix is

$$\begin{aligned} \lambda^3 + P_1\lambda^2 + P_2\lambda + P_3 + e^{-\lambda\tau_1}(Q_1\lambda^2 + Q_2\lambda + Q_3) \\ + e^{-\lambda\tau_2}(R_1\lambda^2 + R_2\lambda + R_3) + e^{-\lambda(\tau_1+\tau_2)}(S_1\lambda + S_2) = 0, \end{aligned} \quad (5.1)$$

where

$$\begin{aligned} P_1 &= -(A_{11} + A_{22} + A_{33}), & P_2 &= A_{11}A_{22} + A_{22}A_{33} + A_{33}A_{11}, \\ P_3 &= -A_{11}A_{22}A_{33}, & Q_1 &= -B_{22}, & Q_2 &= A_{11}B_{22} + A_{33}B_{22} - A_{12}B_{21}, \\ Q_3 &= A_{12}A_{33}B_{21} - A_{11}A_{33}B_{22}, & R_1 &= -C_{33}, & R_2 &= A_{11}C_{33} + A_{22}C_{33} - A_{23}C_{32}, \\ R_3 &= A_{11}A_{23}C_{32} - A_{11}A_{22}C_{33}, & S_1 &= B_{22}C_{33}, & S_2 &= A_{12}B_{21}C_{33} - A_{11}B_{22}C_{33}. \end{aligned}$$

We divide the following analysis into five cases according to the different ranges of values of the two time delays. Based on the characteristic equation (5.1), we analyze the stability of the interior equilibrium point  $E^*$  and the conditions for the occurrence of Hopf-bifurcation, and obtain the following theorems.

**Case 1:**  $\tau_1 = \tau_2 = 0$ .

**Theorem 5.4.** In absence of both delays, the interior equilibrium point  $E^*$  is locally asymptotically stable if  $P_1 + Q_1 + R_1 > 0$ ,  $P_3 + Q_3 + R_3 + S_2 > 0$  and  $(P_1 + Q_1 + R_1)(P_2 + Q_2 + R_2 + S_1) > P_3 + Q_3 + R_3 + S_2$ .

**Case 2:**  $\tau_1 > 0, \tau_2 = 0$ .

**Theorem 5.5.** For system (2.1), when  $\tau_1 > 0, \tau_2 = 0$ , if  $(P_3 + R_3)^2 < (Q_3 + S_2)^2$  holds, the interior equilibrium point  $E^*$  is locally asymptotically stable for all  $\tau_1 \in [0, \tau_{10})$  and unstable for  $\tau_1 > \tau_{10}$ . Furthermore, when  $3\varphi_0^4 + (2E_{11}^2 - 4E_{12} - 2F_{11}^2)\varphi_0^2 + (E_{12}^2 - 2E_{11}E_{13} + 2F_{11}F_{13} - F_{12}^2) > 0$ , then Hopf-bifurcation occurs at  $\tau_1 = \tau_{10}$ , where

$$\begin{aligned} \tau_{10} &= \min_{k,j} \tau_{1k}^{(j)} \\ &= \min_{k,j} \left[ \frac{1}{\varphi_k} \arccos \frac{(E_{11}\varphi_k^2 - E_{13})(F_{13} - F_{11}\varphi_k^2) + F_{12}\varphi_k(\varphi_k^3 - E_{12}\varphi_k)}{(F_{13} - F_{11}\varphi_k^2)^2 + F_{12}^2\varphi_k^2} + \frac{2\pi j}{\varphi_k} \right], \quad k = 1, 2, 3, \quad j = 0, 1, 2, \dots, \end{aligned}$$

and  $\varphi_k$  are defined in the proof.

**Case 3:**  $\tau_1 = 0, \tau_2 > 0$ .

**Theorem 5.6.** For system (2.1), when  $\tau_1 = 0, \tau_2 > 0$ , if  $(P_3 + Q_3)^2 < (R_3 + S_2)^2$  holds, the interior equilibrium point  $E^*$  is locally asymptotically stable for all  $\tau_2 \in [0, \tau_{20})$  and unstable for  $\tau_2 > \tau_{20}$ . Furthermore, when  $3\varphi_0^4 + (2E_{21}^2 - 4E_{22} - 2F_{21}^2)\varphi_0^2 + (E_{22}^2 - 2E_{21}E_{23} + 2F_{21}F_{23} - F_{22}^2) > 0$ , then Hopf-bifurcation occurs at  $\tau_2 = \tau_{20}$ , where

$$\begin{aligned} \tau_{20} &= \min_{k,j} \tau_{2k}^{(j)} \\ &= \min_{k,j} \left[ \frac{1}{\varphi_k} \arccos \frac{(E_{21}\varphi_k^2 - E_{23})(F_{23} - F_{21}\varphi_k^2) + F_{22}\varphi_k(\varphi_k^3 - E_{22}\varphi_k)}{(F_{23} - F_{21}\varphi_k^2)^2 + F_{22}^2\varphi_k^2} + \frac{2\pi j}{\varphi_k} \right], \quad k = 1, 2, 3, \quad j = 0, 1, 2, \dots, \end{aligned}$$

and  $\varphi_k$  are defined in the proof.

**Case 4:**  $\tau_1 > 0, \tau_2 \in (0, \tau_{20})$ .

**Theorem 5.7.** For system (2.1), when  $\tau_1 > 0, \tau_2 \in (0, \tau_{20})$ , if  $(P_3 + R_3)^2 < (Q_3 + S_2)^2$  holds, the interior equilibrium point  $E^*$  is locally asymptotically stable for all  $\tau_1 \in [0, \hat{\tau}_{10})$  and unstable for  $\tau_1 > \hat{\tau}_{10}$ . Furthermore, when  $M_1M_3 + M_2M_4 > 0$ , then Hopf-bifurcation occurs at  $\tau_1 = \hat{\tau}_{10}$ , where

$$\hat{\tau}_{10} = \min_{k,j} \tau_{1k}^{(j)} = \min_{k,j} \frac{1}{\varphi_k} \arccos \frac{\Psi_1\Psi_3 + \Psi_2\Psi_4}{(\Psi_1)^2 + (\Psi_2)^2} + \frac{2\pi j}{\varphi_k}, \quad k = 1, 2, \dots, l; \quad j = 0, 1, 2, \dots$$

and  $\varphi_k$  are defined in the proof.

**Case 5:**  $\tau_1 \in (0, \tau_{10}), \tau_2 > 0$ .

**Theorem 5.8.** For system (2.1), when  $\tau_1 \in (0, \tau_{10}), \tau_2 > 0$ , if  $(P_3 + Q_3)^2 < (R_3 + S_2)^2$  holds, the interior equilibrium point  $E^*$  is locally asymptotically stable for all  $\tau_2 \in [0, \hat{\tau}_{20})$  and unstable for  $\tau_2 > \hat{\tau}_{20}$ . Furthermore, when  $M_5M_7 + M_6M_8 > 0$ , then Hopf-bifurcation occurs at  $\tau_2 = \hat{\tau}_{20}$ , where

$$\hat{\tau}_{20} = \min_{k,j} \tau_{2k}^{(j)} = \min_{k,j} \frac{1}{\varphi_k} \arccos \frac{\Psi_5\Psi_7 + \Psi_6\Psi_8}{(\Psi_5)^2 + (\Psi_6)^2} + \frac{2\pi j}{\varphi_k}, \quad k = 1, 2, \dots, l; \quad j = 0, 1, 2, \dots$$

and  $\varphi_k$  are defined in the proof, where

$$\begin{aligned} M_5 &= \varphi_0^4 - P_2\varphi_0^2 - Q_2\varphi_0 \cos(\varphi_0\tau_1^0) + (-Q_1\varphi_0^2 + Q_3) \sin(\varphi_0\tau_1^0), \\ M_6 &= -P_1\varphi_0^3 + P_3\varphi_0 + (-Q_1\varphi_0^2 + Q_3) \cos(\varphi_0\tau_1^0) + Q_2\varphi_0 \sin(\varphi_0\tau_1^0), \\ M_7 &= 3\varphi_0^3 - P_2 - 2Q_1\varphi_0 \sin(\varphi_0\tau_1^0) - Q_2 \cos(\varphi_0\tau_1^0) - 2R_1\varphi_0 \sin(\varphi_0\tau_2) \\ &\quad - R_2 \cos(\varphi_0\tau_2) + (S_2\tau_1^0 - S_1) \cos(\varphi_0(\tau_1^0 + \tau_2)) + S_1\varphi_0\tau_1^0 \sin(\varphi_0(\tau_1^0 + \tau_2)), \\ M_8 &= -2P_1\varphi_0 - 2Q_1\varphi_0 \cos(\varphi_0\tau_1^0) + Q_2 \sin(\varphi_0\tau_1^0) - 2R_1\varphi_0 \cos(\varphi_0\tau_2) \\ &\quad + R_2 \sin(\varphi_0\tau_2) + S_1\varphi_0\tau_1^0 \cos(\varphi_0(\tau_1^0 + \tau_2)) + (S_1 - S_2\tau_1^0) \sin(\varphi_0(\tau_1^0 + \tau_2)), \\ \Psi_5 &= -R_1\varphi_k^2 + R_3 + S_2 \cos(\varphi_k\tau_1^0) + S_1\varphi_k \sin(\varphi_k\tau_1^0), \\ \Psi_6 &= R_2\varphi_k - S_2 \sin(\varphi_k\tau_1^0) + S_1\varphi_k \cos(\varphi_k\tau_1^0), \\ \Psi_7 &= P_1\varphi_k^2 - P_3 + (Q_1\varphi_k^2 - Q_3) \cos(\varphi_k\tau_1^0) - Q_2\varphi_k \sin(\varphi_k\tau_1^0), \\ \Psi_8 &= \varphi_k^3 - P_2\varphi_k - Q_2\varphi_k \cos(\varphi_k\tau_1^0) + (Q_3 - Q_1\varphi_k^2) \sin(\varphi_k\tau_1^0). \end{aligned}$$

**Remark 1.** The proofs of above theorems are given in the Appendix.

## 6. Numerical simulations

In this section, we use MATLAB R2020a to perform some numerical simulations to illustrate the results of the analysis in the previous sections and plot the corresponding graphs of system (2.1). Since the problem is not a species-specific case study and no real data are available, some hypothetical data are taken here for the simulation.

We make the parameters values  $r = 4.5$ ,  $k = 6$ ,  $b = 0.2$ ,  $a = 0.06$ ,  $\alpha = 1$ ,  $m = 1$ ,  $\beta = 1.3$ ,  $d = 0.03$ ,  $\theta = 4$ ,  $v = 3.1$ ,  $p = 1.14$ ,  $q = 1.13$ ,  $\eta = 2.2$ ,  $e = 0.2$ , and the initial value is  $(\phi_1(s), \phi_2(s), \phi_3(s)) = (2, 2, 2)$ ,  $s \in [-\tau, 0]$ . According to the above parameters, we can obtain all equilibrium points, respectively  $E_0(0, 0, 0)$ ,  $E_1(71.67, 0, 0)$ ,  $E_2(0.0111, 0.4699, 0)$  and  $E^*(14.5, 1.73, 0.51)$ . In the following, we mainly show several cases of interior equilibrium points.

For  $\tau_1 = 0$ ,  $\tau_2 = 0$ , the interior equilibrium point  $E^*$  is locally asymptotically stable (see Figure 1).

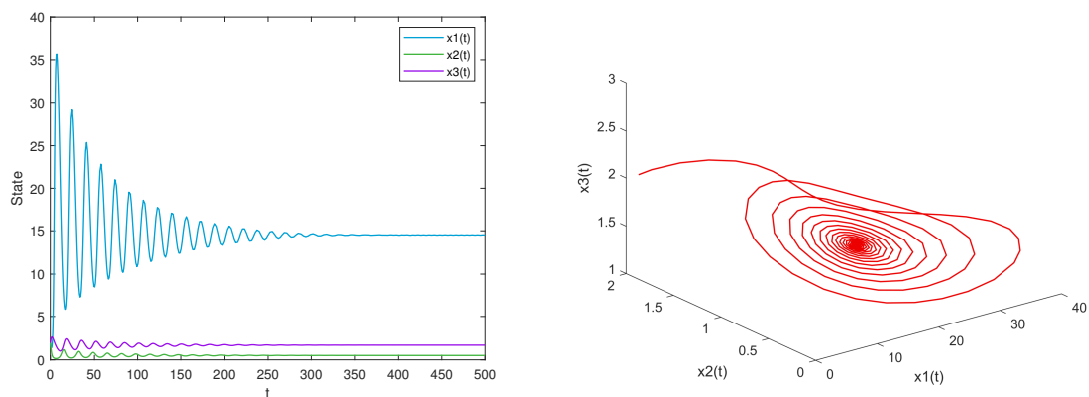


**Figure 1.** The time series and phase portrait of interior equilibrium point  $E^*$  for system (2.1) when  $\tau_1 = 0$  and  $\tau_2 = 0$ .

For  $\tau_1 > 0, \tau_2 = 0$ , we plotted the Hopf-bifurcation diagram Figure 2 concerning  $\tau_1$ . If we change the value of  $\tau_1$  from 0 to 14, then the system undergoes Hopf-bifurcation. Hence, the interior equilibrium  $E^*$  is locally asymptotically stable for  $\tau_1 = 1 < \tau_{10} \approx 10.88$  (see Figure 3) and unstable for  $\tau_1 = 13 > \tau_{10} \approx 10.88$  (see Figure 4).

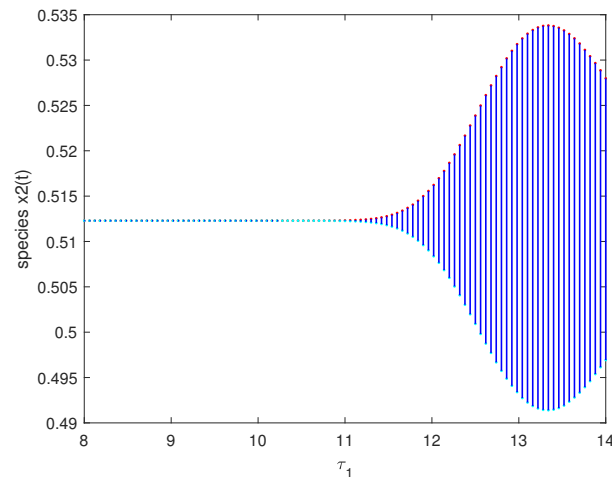


**Figure 2.** The Hopf-bifurcation diagram for system (2.1) with respect to  $\tau_1$  when  $\tau_2 = 0$ .

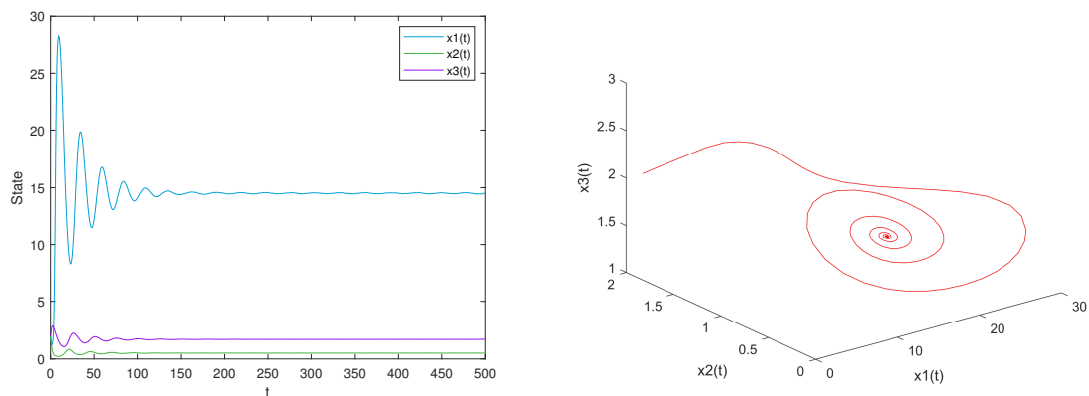


**Figure 3.** When  $\tau_2 = 0$ ,  $E^*$  is locally asymptotically stable for  $\tau_1 = 1 < \tau_{10} \approx 10.88$ .

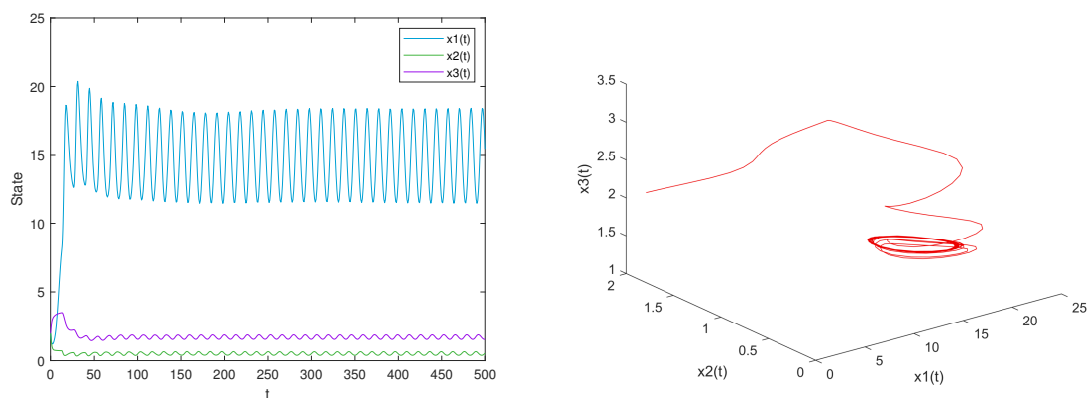


**Figure 4.** When  $\tau_2 = 0$ ,  $E^*$  undergoes a Hopf-bifurcation for  $\tau_1 = 13 > \hat{\tau}_{10} \approx 10.88$ .

For  $\tau_1 = 0, \tau_2 > 0$ , if we continuously increase the value of  $\tau_2$ , we can find a critical value of  $\tau_{20}$ , namely  $\tau_{20} \approx 0.11$  for which system (2.1) undergoes Hopf-bifurcation (see Figure 5). Hence,  $E^*$  is locally asymptotically stable for  $\tau_2 = 0.1 < \tau_{20} \approx 0.11$  (see Figure 6) and unstable for  $\tau_2 = 0.2 > \tau_{20} \approx 0.11$  (see Figure 7).

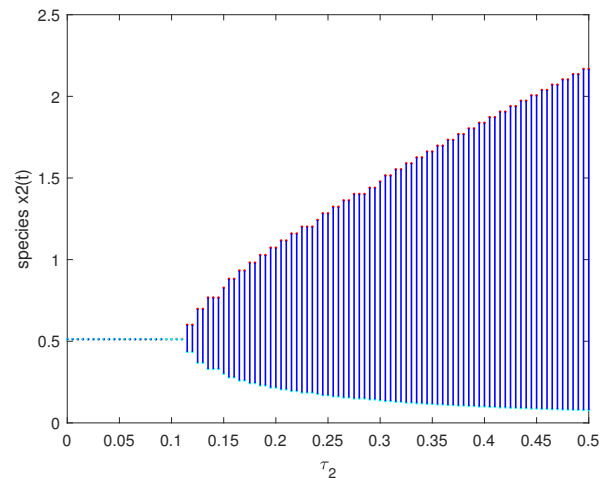


**Figure 5.** The Hopf-bifurcation diagram for system (2.1) with respect to  $\tau_2$  when  $\tau_1 = 0$ .

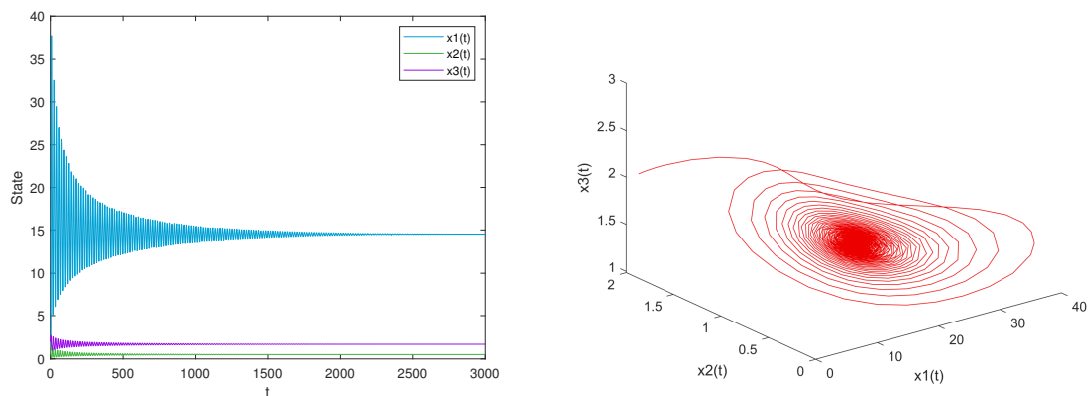


**Figure 6.** When  $\tau_1 = 0$ ,  $E^*$  is locally asymptotically stable for  $\tau_2 = 0.1 < \tau_{20} \approx 0.11$ .

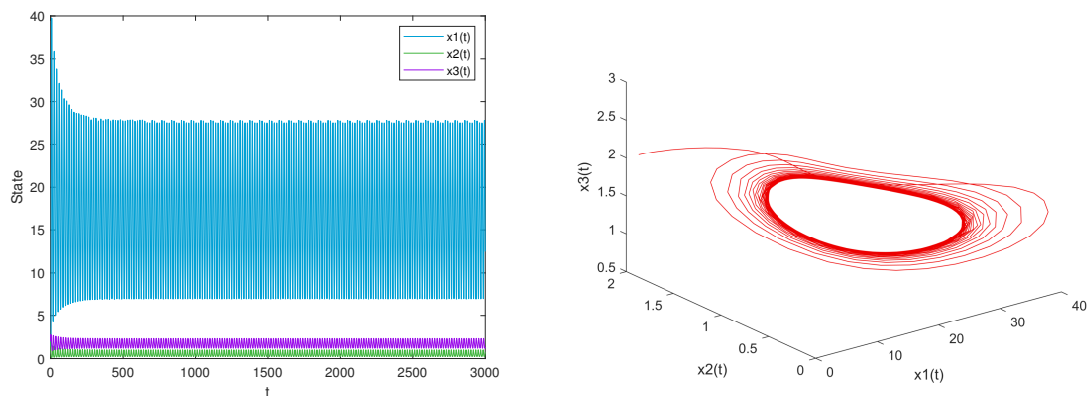


**Figure 7.** When  $\tau_1 = 0$ ,  $E^*$  undergoes a Hopf-bifurcation for  $\tau_2 = 0.2 > \hat{\tau}_{20} \approx 0.11$ .

For  $\tau_1 > 0$ , fixing  $\tau_2 = 0.1 \in (0, \tau_{20})$ , we get  $\hat{\tau}_{10} \approx 10.28$ , so when  $\tau_1 = 2 < \hat{\tau}_{10}$ ,  $E^*$  is locally asymptotically stable (see Figure 8), when  $\tau_1 = 12 > \hat{\tau}_{10}$ ,  $E^*$  is unstable (see Figure 9). Then Hopf-bifurcation occurs at  $\hat{\tau}_{10} \approx 10.28$  (see Figure 10).

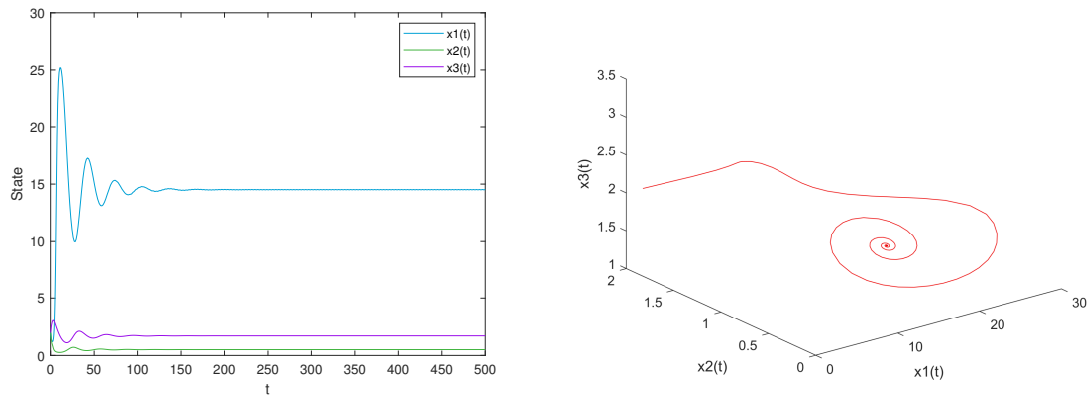


**Figure 8.** Fixing  $\tau_2 = 0.1 \in (0, \tau_{20})$ , when  $\tau_1 = 2 < \hat{\tau}_{10}$ ,  $E^*$  is locally asymptotically stable.

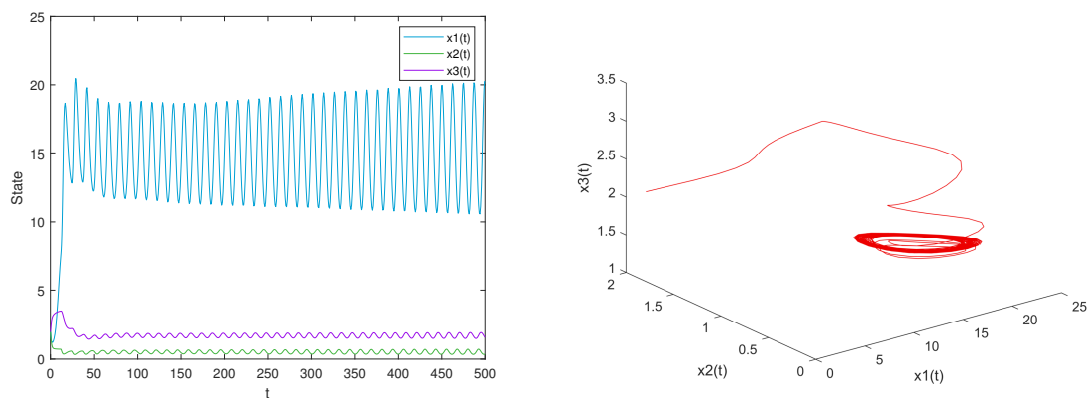


**Figure 9.** Fixing  $\tau_2 = 0.1 \in (0, \tau_{20})$ , when  $\tau_1 = 12 > \hat{\tau}_{10}$ ,  $E^*$  undergoes a Hopf-bifurcation.

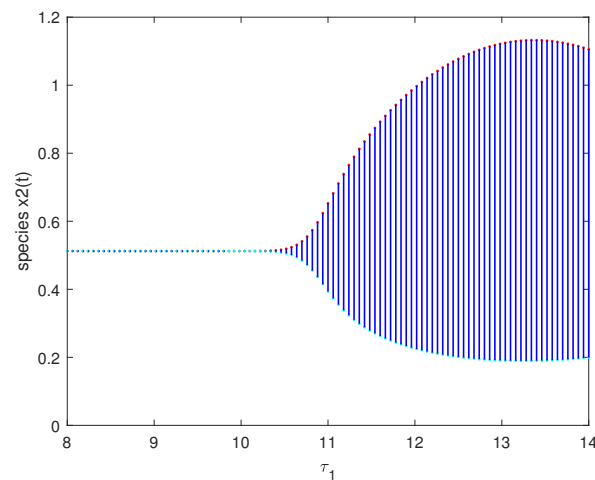


**Figure 10.** The Hopf-bifurcation diagram for system (2.1) with respect to  $\tau_1$  when  $\tau_2 = 0.1$ .

For  $\tau_2 > 0$ , fixing  $\tau_1 = 1 \in (0, \tau_{10})$ , we get  $\hat{\tau}_{20} \approx 0.96$ , so when  $\tau_2 = 0.1 < \hat{\tau}_{20}$ ,  $E^*$  is locally asymptotically stable (see Figure 11), when  $\tau_2 = 1.1 > \hat{\tau}_{20}$ ,  $E^*$  is unstable (see Figure 12). Then Hopf bifurcation occurs at  $\hat{\tau}_{20} \approx 0.96$  (see Figure 13).

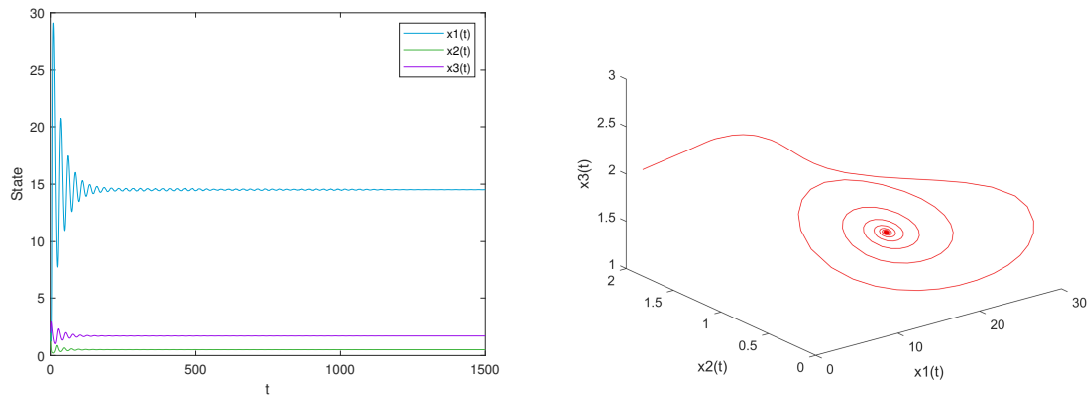


**Figure 11.** Fixing  $\tau_1 = 1 \in (0, \tau_{10})$ , when  $\tau_2 = 0.1 < \hat{\tau}_{20}$ ,  $E^*$  is locally asymptotically stable.

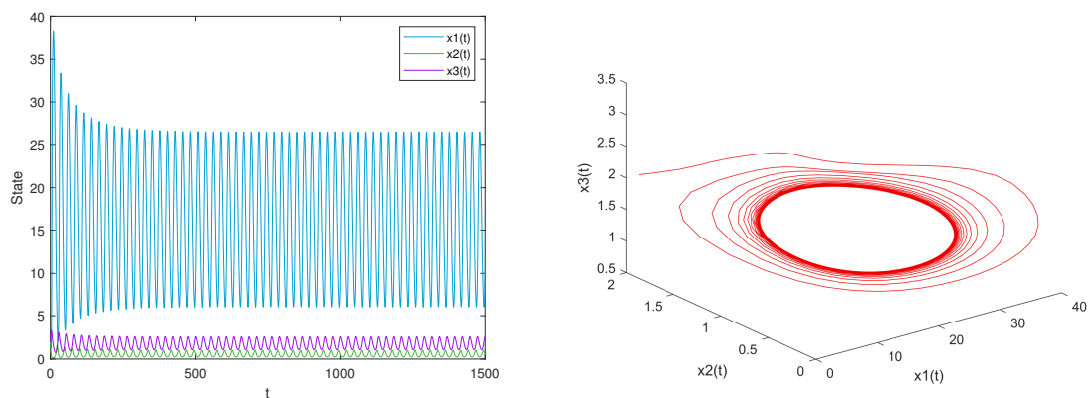


**Figure 12.** Fixing  $\tau_1 = 1 \in (0, \tau_{10})$ , when  $\tau_2 = 1.1 > \hat{\tau}_{20}$ ,  $E^*$  undergoes a Hopf-bifurcation.

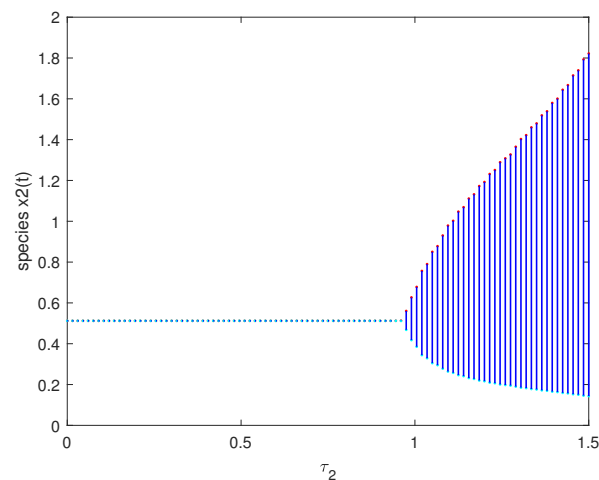


**Figure 13.** The Hopf-bifurcation diagram for system (2.1) with respect to  $\tau_2$  when  $\tau_1 = 1$ .

Based on above analysis, we summarize the dynamics of the interior equilibrium  $E^*$  of system (2.1) in Table 1.

**Table 1.** The effect of delays on the stability of the interior equilibrium  $E^*$  of system (2.1).

Values of delay	Thresholds of delay	Simulation results	Explanations of simulation
$\tau_2 = 0$	$\tau_{10} \approx 10.88$	Figure 2	When $\tau_2 = 0$ , $E^*$ is locally asymptotically stable for $\tau_1 < 10.88$ and unstable for $\tau_1 > 10.88$ .
$\tau_1 = 0$	$\tau_{20} \approx 0.11$	Figure 5	When $\tau_1 = 0$ , $E^*$ is locally asymptotically stable for $\tau_2 < 0.11$ and unstable for $\tau_2 > 0.11$ .
$\tau_2 = 0.1 \in (0, \tau_{20})$	$\hat{\tau}_{10} \approx 10.28$	Figure 10	When $\tau_2 = 0.1 \in (0, \tau_{20})$ , $E^*$ is locally asymptotically stable for $\tau_1 < 10.28$ and unstable for $\tau_1 > 10.28$ .
$\tau_1 = 1 \in (0, \tau_{10})$	$\hat{\tau}_{20} \approx 0.96$	Figure 13	When $\tau_1 = 1 \in (0, \tau_{10})$ , $E^*$ is locally asymptotically stable for $\tau_2 < 0.96$ and unstable for $\tau_2 > 0.96$ .

Finally we investigate how the fear of predators affect the population dynamics. By increasing the fear values and taking  $k = 6, 9, 15$  and  $20$  respectively, we plot the time series graphs of each species (see Figures 14–16).

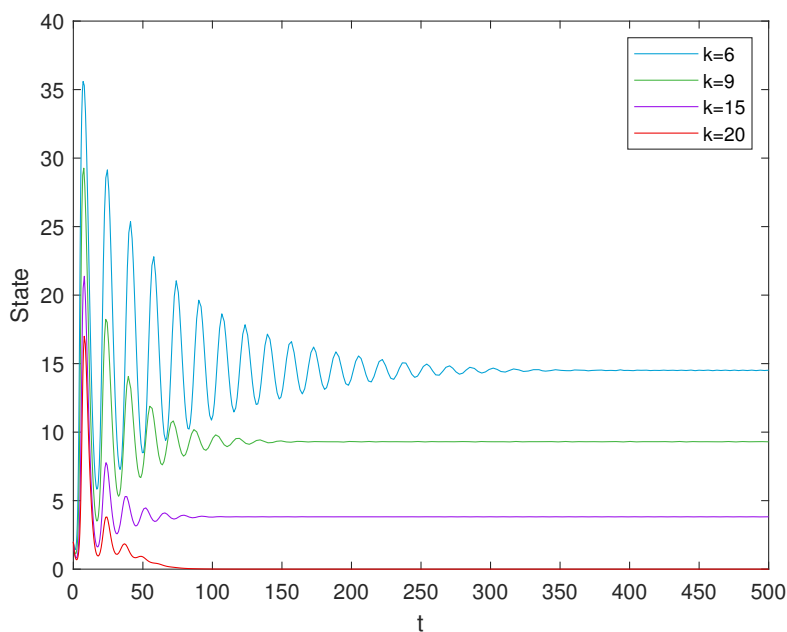


**Figure 14.** The influence of different degrees of fear  $k$  on  $x_1(t)$ .

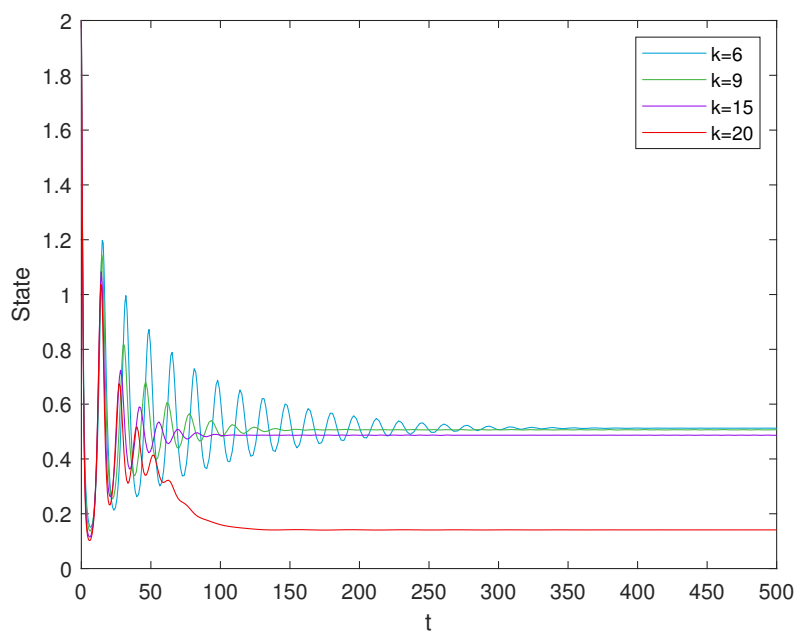


**Figure 15.** The influence of different degrees of fear  $k$  on  $x_2(t)$ .

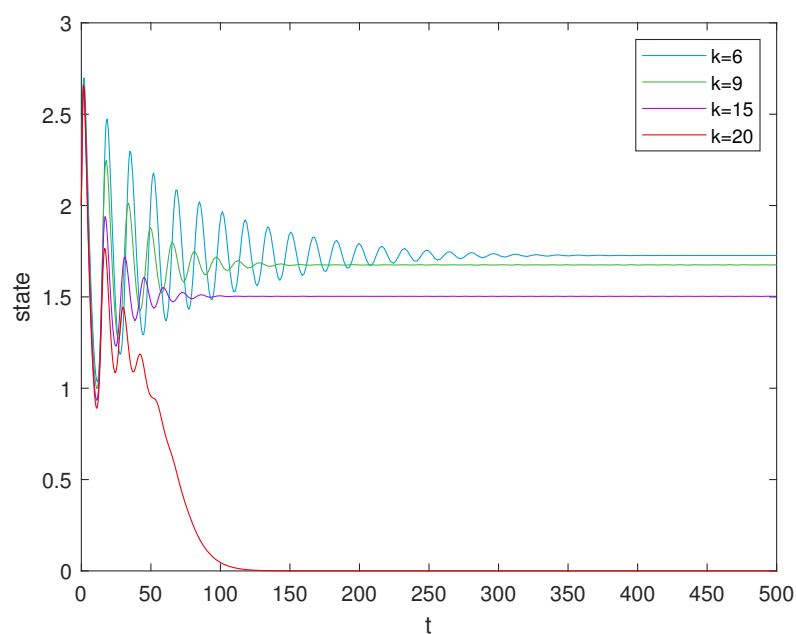


**Figure 16.** The influence of different degrees of fear  $k$  on  $x_3(t)$ .

(1) The effect of fear on prey. In Figure 14, we observe that fear inhibits prey reproduction and excessive fear leads to prey extinction.

(2) The effect of fear on intermediate predators. In Figure 15, we observe that an increase in the value of fear leads to a shorter duration of intermediate predator turbulence, but little change in the

number of species, and too much fear leads to a decrease and stabilization of the number of species.

(3) The effect of fear on the top predator. In Figure 16, an increase in fear leads to a decrease in the turbulence time of the highest predator and a decrease in the number of species, and too much fear leads the highest predator to extinction.

## 7. Discussion and conclusions

In this paper, we analyze the dynamics of a three-chain model containing indirect predation (fear of predator) and two delays, where the three species are the prey, intermediate predator and top predator, and the two delays represent the gestation delays of the intermediate and top predator, respectively.

First, we investigate the positivity and boundedness of this system, where boundedness can be seen as a natural limit to expansion due to limited resources and positivity implies that species persist. Next, we study the effect of delay on the stability of the model by varying the delay parameters  $\tau_1$  and  $\tau_2$ . According to the theorem in Section 5, we obtain the conditions when the system is stable. By selecting appropriate parameter values, we draw the Hopf-bifurcation diagrams (Figures 2, 5, 10 and 13), that is, if  $\tau$  increases continuously, a threshold  $\tau_0$  will be obtained. If  $\tau < \tau_0$ , the system is stable; otherwise, the system becomes unstable, that is, a Hopf-bifurcation occurs at  $\tau = \tau_0$ . These observations confirm the important role of delay in the system. Through numerical simulations, we find that fear may reduce the number of species and even lead to extinction of species. Thus, fear has an important influence on the dynamics of predator-prey systems.

In nature, in addition to fear, other factors such as refuge, additional food, and human capture influence the predator-prey system. As a part of future research on the model in this paper, the inclusion of refuge and human capture could be considered to make the model more realistic. Moreover, for the discrete-time model [6, 7] and the infectious disease model [8], we believe there will be some interesting findings. All these will be left to our future work.

## Acknowledgments

The authors would like to thank the referees for their suggestions and valuable comments, which have greatly improved the presentation of this paper.

This work is funded by NSF of China (No. 11861027).

## Conflict of interest

The authors declare that they have no competing interests in this paper.

## Appendix

Here, we give the proofs of Theorems 5.1 to 5.8.

### Proof of Theorem 5.1:

*Proof.* Based on the eigenvalues less than 0, we obtain that  $E_0$  is locally asymptotically stable when  $r < b$ . □

**Proof of Theorem 5.2:**

*Proof.* By calculating the Jacobian matrix at the equilibrium  $E_1$ , we obtain

$$J_{E_1} = \begin{bmatrix} -(r-b) & -kr\frac{r-b}{a} - \alpha & 0 \\ 0 & -d + \beta e^{-\lambda\tau_1} & 0 \\ 0 & 0 & -e \end{bmatrix}.$$

Obviously, we get  $\lambda_1 = -(r-b) < 0$ ,  $\lambda_2 = -e < 0$ , and the other eigenvalue is the root of the following equation:

$$-d + \beta e^{-\lambda\tau_1} - \lambda = 0. \quad (\text{A.1})$$

In the absence of delay, i.e. when  $\tau_1 = 0$ ,  $E_1$  is locally asymptotically stable if  $\beta < d$ .

When  $\tau_1 > 0$  and  $\beta < d$ , we assume that  $\lambda = \xi + i\varphi$  ( $\xi, \varphi \in \mathbb{R}$ ) is the root of Eq (A.1). Then substituting the value of  $\lambda$  into Eq (A.1) and separating the real and imaginary parts, we obtain

$$\beta e^{-\xi\tau_1} \cos(\varphi\tau_1) - d - \xi = 0, \quad (\text{A.2})$$

$$\beta e^{-\xi\tau_1} + \varphi = 0. \quad (\text{A.3})$$

To eliminate  $\tau_1$ , we square and add the Eqs (A.2) and (A.3), and obtain the following equation

$$\varphi^2 = \beta^2 e^{-2\xi\tau_1} - (d - \xi)^2,$$

$$\text{i.e., } \varphi = \pm \sqrt{(\beta e^{-\xi\tau_1} + d + \xi)(\beta e^{-\xi\tau_1} - d - \xi)}.$$

Let  $\xi \geq 0$ , then  $(\beta e^{-\xi\tau_1} - d - \xi) \leq (\beta - d - \xi) < 0$ . Thus, if  $\xi \geq 0$ , no such real  $\varphi$  exists, which contradicts the previous assumption  $\varphi \in \mathbb{R}$ . So  $\xi < 0$ , i.e., the Eq (A.1) contains a negative real root and an imaginary root with a negative real part (if exists).

Therefore,  $E_1$  is locally asymptotically stable if  $\beta < d$ .  $\square$

**Proof of Theorem 5.3:**

*Proof.* The Jacobian matrix at  $E_2$  is:

$$J_{E_2} = \begin{bmatrix} -a\bar{x}_1 + \frac{\alpha\bar{x}_1\bar{x}_2}{(\bar{x}_1+m\bar{x}_2)^2} & -\frac{kr\bar{x}_1}{(1+k\bar{x}_2)^2} - \frac{\alpha\bar{x}_1^2}{(\bar{x}_1+m\bar{x}_2)^2} & 0 \\ \frac{\beta m\bar{x}_2^2}{(\bar{x}_1+m\bar{x}_2)^2} e^{-\lambda\tau_1} & -d + \frac{\beta\bar{x}_1^2}{(\bar{x}_1+m\bar{x}_2)^2} e^{-\lambda\tau_1} & -\frac{\theta\bar{x}_2}{v+p\bar{x}_2} \\ 0 & 0 & -e + \frac{\eta\bar{x}_2}{v+p\bar{x}_2} e^{-\lambda\tau_2} \end{bmatrix}.$$

The characteristic equation of above matrix  $J_{E_2}$  is given by  $\det(J_{E_2} - \lambda I) = 0$ .

One root of  $\det(J_{E_2} - \lambda I) = 0$  is given by  $-e + \frac{\eta\bar{x}_2}{v+p\bar{x}_2} e^{-\lambda\tau_2} - \lambda = 0$ . The analysis process is similar to Eq (A.1). Therefore, if  $-e + \frac{\eta\bar{x}_2}{v+p\bar{x}_2} < 0$ , i.e.,  $\bar{x}_2 < \frac{ve}{\eta-pe}$ , then the equation contains negative real roots and imaginary roots with negative real parts (if exists).

The other two eigenvalues are the root of the quadratic equation

$$\lambda^2 + H_1\lambda + H_2 + e^{-\lambda\tau_1}(N_1\lambda + N_2) = 0, \quad (\text{A.4})$$

where

$$H_1 = a\bar{x}_1 + d - \frac{\alpha\bar{x}_1\bar{x}_2}{(\bar{x}_1 + m\bar{x}_2)^2},$$

$$\begin{aligned}
 H_2 &= -d \left( -a\bar{x}_1 + \frac{\alpha\bar{x}_1\bar{x}_2}{(\bar{x}_1 + m\bar{x}_2)^2} \right), \\
 N_1 &= \frac{\beta\bar{x}_1^2}{(\bar{x}_1 + m\bar{x}_2)^2}, \\
 N_2 &= \frac{\beta\bar{x}_1^2}{(\bar{x}_1 + m\bar{x}_2)^2} \left( -a\bar{x}_1 + \frac{\alpha\bar{x}_1\bar{x}_2}{(\bar{x}_1 + m\bar{x}_2)^2} \right) + \frac{\beta m\bar{x}_2^2}{(\bar{x}_1 + m\bar{x}_2)^2} \left( \frac{k r \bar{x}_1}{(1 + k\bar{x}_2)^2} + \frac{\alpha\bar{x}_1^2}{(\bar{x}_1 + m\bar{x}_2)^2} \right).
 \end{aligned}$$

**Case 1:**  $\tau_1 = 0$ , then Eq (A.4) becomes

$$\lambda^2 + (H_1 + N_1)\lambda + H_2 + N_2 = 0. \quad (\text{A.5})$$

According to Routh-Hurwitz criteria, both roots of the Eq (A.5) are negative real parts if  $(H_2 + N_2) > 0$  and  $(H_1 + N_1) > 0$ , i.e.  $\left(-a\bar{x}_1 + \frac{\alpha\bar{x}_1\bar{x}_2}{(\bar{x}_1 + m\bar{x}_2)^2}\right) \left(\frac{\beta\bar{x}_1^2}{(\bar{x}_1 + m\bar{x}_2)^2} - d\right) + \frac{\beta m\bar{x}_2^2}{(\bar{x}_1 + m\bar{x}_2)^2} \left(\frac{k r \bar{x}_1}{(1 + k\bar{x}_2)^2} + \frac{\alpha\bar{x}_1^2}{(\bar{x}_1 + m\bar{x}_2)^2}\right) > 0$  and  $a\bar{x}_1 + d + \frac{\beta\bar{x}_1^2}{(\bar{x}_1 + m\bar{x}_2)^2} > \frac{\alpha\bar{x}_1\bar{x}_2}{(\bar{x}_1 + m\bar{x}_2)^2}$ .

**Case 2:**  $\tau_1 > 0$  and  $\bar{x}_2 < \frac{ve}{\eta - pe}$ . By substituting  $\lambda = \xi + i\varphi$  into Eq (A.4) and separating the real and imaginary parts, we have

$$\xi^2 - \varphi^2 + H_1\xi + H_2 + e^{-\xi\tau_1} [(N_1\xi + N_1N_2) \cos(\varphi\tau_1) + N_1\varphi \sin(\varphi\tau_1)] = 0, \quad (\text{A.6})$$

$$2\xi\varphi + H_1\varphi + e^{-\xi\tau_1} [N_1\varphi \cos(\varphi\tau_1) - (N_1\xi + N_1N_2) \sin(\varphi\tau_1)] = 0. \quad (\text{A.7})$$

Putting  $\xi = 0$ , Eqs (A.6) and (A.7) become

$$N_2 \cos(\varphi\tau_1) + N_1 \sin(\varphi\tau_1) = \varphi^2 - H_2, \quad (\text{A.8})$$

$$N_1\varphi \cos(\varphi\tau_1) - N_2 \sin(\varphi\tau_1) = -H_1\varphi. \quad (\text{A.9})$$

By squaring and adding, we obtain

$$\varphi^4 + (H_1^2 - 2H_2 - N_1^2)\varphi^2 + H_2^2 - N_2^2 = 0. \quad (\text{A.10})$$

Using Descartes's rule of sign, the equation has at least one positive root  $\varphi_0$  if  $H_2^2 - N_2^2 < 0$ . By calculating (A.8) and (A.9), we get

$$\tau_{1j} = \frac{1}{\varphi_0} \arccos \left[ \frac{N_2(\varphi_0^2 - H_2) - H_1 N_1 \varphi_0^2}{N_1^2 \varphi_0^2 + N_2^2} \right] + \frac{2\pi j}{\varphi_0} \quad j = 0, 1, 2, \dots \quad (\text{A.11})$$

Let  $\hat{\tau}_1 = \min_{j=0,1,2,\dots} \tau_{1j}$ .

Now the transversality condition  $Re \left( \frac{d\lambda}{d\tau_1} \right)_{\lambda=i\varphi_0}^{-1} > 0$  will be verified.

By differentiating Eq (A.4) with respect to  $\tau_1$ , we obtain

$$\left( \frac{d\lambda}{d\tau_1} \right)^{-1} = -\frac{2\lambda + H_1}{\lambda(\lambda^2 + H_1\lambda + H_2)} + \frac{N_1}{\lambda(N_1\lambda + N_2)} - \frac{\tau_1}{\lambda},$$

which leads to

$$\begin{aligned} \operatorname{Re}\left(\frac{d\lambda}{d\tau_1}\right)^{-1}_{\lambda=i\varphi_0} &= \operatorname{Re}\left(-\frac{2\lambda + H_1}{\lambda(\lambda^2 + H_1\lambda + H_2)}\right)_{\lambda=i\varphi_0} + \operatorname{Re}\left(\frac{N_1}{\lambda(N_1\lambda + N_2)}\right)_{\lambda=i\varphi_0} \\ &= \frac{H_1^2 + 2(\varphi_0^2 - H_2)}{H_1^2\varphi_0^2 + (\varphi_0^2 - H_2)^2} - \frac{N_1^2}{N_1^2\varphi_0^2 + N_2^2}. \end{aligned}$$

From (A.10), we have

$$H_1^2\varphi_0^2 + (\varphi_0^2 - H_2)^2 = N_1^2\varphi_0^2 + N_2^2.$$

Then

$$\operatorname{Re}\left(\frac{d\lambda}{d\tau_1}\right)^{-1}_{\lambda=i\varphi_0} = \frac{H_1^2 - N_1^2 + 2(\varphi_0^2 - H_2)}{H_1^2\varphi_0^2 + (\varphi_0^2 - H_2)^2} = \frac{2\varphi_0^2 + H_1 - N_1^2 - 2H_2}{H_1^2\varphi_0^2 + (\varphi_0^2 - H_2)^2}.$$

When  $2\varphi_0^2 + H_1 - N_1^2 - 2H_2 > 0$ ,  $\operatorname{Re}\left(\frac{d\lambda}{d\tau_1}\right)^{-1}_{\lambda=i\varphi_0} > 0$ . Therefore, the transversality condition is satisfied and a Hopf-bifurcation occurs at  $E_2$  for  $\tau_1 = \hat{\tau}_1$ .  $\square$

#### Proof of Theorem 5.4:

*Proof.* The characteristic (5.1) becomes

$$\lambda^3 + (P_1 + Q_1 + R_1)\lambda^2 + (P_2 + Q_2 + R_2 + S_1)\lambda + P_3 + Q_3 + R_3 + S_2 = 0. \quad (\text{A.12})$$

Therefore, by Routh-Hurwitz Criteria, we obtain all the roots of (A.12) have negative real part, if  $P_1 + Q_1 + R_1 > 0$ ,  $P_3 + Q_3 + R_3 + S_2 > 0$  and  $(P_1 + Q_1 + R_1)(P_2 + Q_2 + R_2 + S_1) > P_3 + Q_3 + R_3 + S_2$ . This means that the interior equilibrium  $E^*$  is locally asymptotically stable.  $\square$

#### Proof of Theorem 5.5:

*Proof.* The characteristic (5.1) becomes

$$\lambda^3 + E_{11}\lambda^2 + E_{12}\lambda + E_{13} + e^{-\lambda\tau_1}(F_{11}\lambda^2 + F_{12}\lambda + F_{13}) = 0, \quad (\text{A.13})$$

where  $E_{11} = P_1 + R_1$ ,  $E_{12} = P_2 + R_2$ ,  $E_{13} = P_3 + R_3$ ,  $F_{11} = Q_1$ ,  $F_{12} = Q_2 + S_1$ ,  $F_{13} = Q_3 + S_2$ . Let  $\lambda = \xi + i\varphi$  be the root of (A.13). Then we obtain

$$\begin{aligned} \xi^3 - 3\xi\varphi^2 + E_{11}\xi^2 - E_{11}\varphi^2 + E_{12}\xi + E_{13} + e^{-\xi\tau_1}[(F_{11}\xi^2 - F_{11}\varphi^2 \\ + F_{12}\xi + F_{13})\cos(\varphi\tau_1) + (2F_{11}\xi\varphi + F_{12}\varphi)\sin(\varphi\tau_1)] &= 0, \\ -\varphi^3 + 3\xi^2\varphi + 2E_{11}\xi\varphi + E_{12}\varphi + e^{-\xi\tau_1}[(2F_{11}\xi\varphi + F_{12}\varphi)\cos(\varphi\tau_1) \\ - (F_{11}\xi^2 - F_{11}\varphi^2 + F_{12}\xi + F_{13})\sin(\varphi\tau_1)] &= 0. \end{aligned}$$

A necessary condition for changing the stability of the equilibrium point  $E^*$  is that the real part of the root of the Eq (A.13) changes the sign. To find the stable switching point, we consider  $\xi = 0$ , then we have

$$(F_{13} - F_{11}\varphi^2)\cos(\varphi\tau_1) + F_{12}\varphi\sin(\varphi\tau_1) = E_{11}\varphi^2 - E_{13}, \quad (\text{A.14})$$

$$F_{12}\varphi \cos(\varphi\tau_1) + (F_{11}\varphi^2 - F_{13})\sin(\varphi\tau_1) = \varphi^3 - E_{12}\varphi. \quad (\text{A.15})$$

By squaring and adding (A.14) and (A.15), we obtain

$$\varphi^6 + K_{11}\varphi^4 + K_{12}\varphi^2 + K_{13} = 0, \quad (\text{A.16})$$

where  $K_{11} = E_{11}^2 - 2E_{12} - F_{11}$ ,  $K_{12} = E_{12}^2 - 2E_{11}E_{13} + 2F_{11}F_{13} - F_{12}^2$ ,  $K_{13} = E_{13}^2 - F_{13}^2$ .

Let  $\varphi^2 = \sigma$ , we get

$$h_1(\sigma) = \sigma^3 + K_{11}\sigma^2 + K_{12}\sigma + K_{13} = 0. \quad (\text{A.17})$$

Then,  $h_1(0) = K_{13} = E_{13}^2 - F_{13}^2 = (P_3 + R_3)^2 - (Q_3 + S_2)^2$  and  $\lim_{\sigma \rightarrow \infty} h_1(\sigma) = +\infty$ . We assume that  $h_1(0) < 0 \Rightarrow (P_3 + R_3)^2 < (Q_3 + S_2)^2$ . According to Descartes's rule of sign, the Eq (A.17) has at least one positive root and can have at most three positive roots.

Without loss of generality, we assume that it has three positive roots, denoted by  $\varphi_k = \sqrt{\sigma_k}$  and  $k = 1, 2, 3$ . By calculating (A.14) and (A.15), we obtain

$$\tau_{1k}^j = \frac{1}{\varphi_k} \arccos \frac{(E_{11}\varphi_k^2 - E_{13})(F_{13} - F_{11}\varphi_k^2) + F_{12}\varphi_k(\varphi_k^3 - E_{12}\varphi_k)}{(F_{13} - F_{11}\varphi_k^2)^2 + F_{12}^2\varphi_k^2} + \frac{2\pi j}{\varphi_k}$$

where  $k = 1, 2, 3$  and  $j = 0, 1, 2, \dots$ . Let  $\tau_{10} = \min_{k,j} \tau_{1k}^{(j)}$ ,  $k = 1, 2, 3$ ,  $j = 0, 1, 2, \dots$

Now the transversality condition  $Re \left( \frac{d\lambda}{d\tau_1} \right)_{\lambda=i\varphi_0}^{-1} > 0$  will be verified.

By differentiating Eq (A.13) with respect to  $\tau_1$ , we obtain

$$\left( \frac{d\lambda}{d\tau_1} \right)^{-1} = -\frac{3\lambda^2 + 2E_{11}\lambda + E_{12}}{\lambda(\lambda^3 + E_{11}\lambda^2 + E_{12}\lambda + E_{13})} + \frac{2F_{11}\lambda + F_{12}}{\lambda(F_{11}\lambda^2 + F_{12}\lambda + F_{13})} - \frac{\tau_1}{\lambda},$$

which leads to

$$Re \left( \frac{d\lambda}{d\tau_1} \right)_{\lambda=i\varphi_0}^{-1} = \frac{3\varphi_0^4 + (2E_{11}^2 - 4E_{12})\varphi_0^2 + (E_{12}^2 - 2E_{11}E_{13})}{\varphi_0^6 + (E_{11}^2 - 2E_{12})\varphi_0^4 + (E_{12}^2 - 2E_{11}E_{13})\varphi_0^2 + E_{13}^2} + \frac{-2F_{11}^2\varphi_0^2 + (2F_{11}F_{13} - F_{12}^2)}{F_{11}^2\varphi_0^4 + (F_{12}^2 - 2F_{11}F_{13})\varphi_0^2 + F_{13}^2}.$$

From (A.16), we have

$$\varphi_0^6 + (E_{11}^2 - 2E_{12})\varphi_0^4 + (E_{12}^2 - 2E_{11}E_{13})\varphi_0^2 + E_{13}^2 = F_{11}^2\varphi_0^4 + (F_{12}^2 - 2F_{11}F_{13})\varphi_0^2 + F_{13}^2.$$

Then

$$Re \left( \frac{d\lambda}{d\tau_1} \right)_{\lambda=i\varphi_0}^{-1} = \frac{3\varphi_0^4 + (2E_{11}^2 - 4E_{12} - 2F_{11}^2)\varphi_0^2 + (E_{12}^2 - 2E_{11}E_{13} + 2F_{11}F_{13} - F_{12}^2)}{\varphi_0^6 + (E_{11}^2 - 2E_{12})\varphi_0^4 + (E_{12}^2 - 2E_{11}E_{13})\varphi_0^2 + E_{13}^2}.$$

When  $3\varphi_0^4 + (2E_{11}^2 - 4E_{12} - 2F_{11}^2)\varphi_0^2 + (E_{12}^2 - 2E_{11}E_{13} + 2F_{11}F_{13} - F_{12}^2) > 0$ ,  $Re \left( \frac{d\lambda}{d\tau_1} \right)_{\lambda=i\varphi_0}^{-1} > 0$ . Therefore, the transversality condition is satisfied and a Hopf-bifurcation occurs around when  $\tau_1$  passes through the critical value  $\tau_{10}$ .  $\square$

### Proof of Theorem 5.6:

*Proof.* The characteristic (5.1) becomes

$$\lambda^3 + E_{21}\lambda^2 + E_{22}\lambda + E_{23} + e^{-\lambda\tau_2}(F_{21}\lambda^2 + F_{22}\lambda + F_{23}) = 0,$$

where  $E_{21} = P_1 + Q_1$ ,  $E_{22} = P_2 + Q_2$ ,  $E_{23} = P_3 + Q_3$ ,  $F_{21} = Q_1$ ,  $F_{22} = R_2 + S_1$ ,  $F_{23} = R_3 + S_2$ .

The calculation process is similar to Theorem 5.5.  $\square$

### Proof of Theorem 5.7:

*Proof.* We consider that  $\tau_2 = \tau_2^0$  in its stable interval, with  $\tau_1$  as the parameter.

Let  $\lambda = \xi + i\varphi$  be the root of (5.1), we get

$$\begin{aligned} & \xi^3 - 3\xi\varphi^2 + P_1\xi^2 - P_1\varphi^2 + P_2\xi + P_3 + e^{-\xi\tau_1}[(Q_1\xi^2 - Q_1\varphi^2 + Q_2\xi + Q_3)\cos(\varphi\tau_1) \\ & + (2Q_1\xi\varphi + Q_2\varphi)\sin(\varphi\tau_1)] + e^{-\xi\tau_2^0}[(R_1\xi^2 - R_1\varphi^2 + R_2\xi + R_3)\cos(\varphi\tau_2^0) + (2R_1\xi\varphi \\ & + R_2\varphi)\sin(\varphi\tau_2^0)] + e^{-\xi(\tau_1+\tau_2^0)}[(S_1\xi + S_2)\cos(\varphi(\tau_1 + \tau_2^0)) + S_1\varphi\sin(\varphi(\tau_1 + \tau_2^0))] = 0, \\ & 3\xi^2\varphi - \varphi^3 + 2P_1\xi\varphi + P_2\varphi + e^{-\xi\tau_1}[(2Q_1\xi\varphi + Q_2\varphi)\cos(\varphi\tau_1) - (Q_1\xi^2 - Q_1\varphi^2 + Q_2\xi + Q_3) \\ & \times \sin(\varphi\tau_1)] + e^{-\xi\tau_2^0}[(2R_1\xi\varphi + R_2\varphi)\cos(\varphi\tau_2^0) - (R_1\xi^2 - R_1\varphi^2 + R_2\xi + R_3)\sin(\varphi\tau_2^0)] \\ & + e^{-\xi(\tau_1+\tau_2^0)}[S_1\varphi\cos(\varphi(\tau_1 + \tau_2^0)) + (S_1\xi + S_2)\sin(\varphi(\tau_1 + \tau_2^0))] = 0. \end{aligned}$$

A necessary condition for the stability change of the equilibrium point  $E^*$  is that the characteristic Eq (5.1) has a pair of purely imaginary roots, i.e.,  $\xi = 0$ . Let  $\xi = 0$ , and we obtain

$$\begin{aligned} & [-Q_1(\varphi)^2 + Q_3 + S_2\cos(\varphi\tau_2^0) + S_1\varphi\sin(\varphi\tau_2^0)]\cos(\varphi\tau_1) \\ & + [Q_2\varphi - S_2\sin(\varphi\tau_2^0) + S_1\cos(\varphi\tau_2^0)]\sin(\varphi\tau_1) \tag{A.18} \\ & = P_1(\varphi)^3 - P_3 + (R_1\varphi - R_3)\cos(\varphi\tau_2^0) - R_2\varphi\sin(\varphi\tau_2^0), \end{aligned}$$

$$\begin{aligned} & [Q_2\varphi - S_2\sin(\varphi\tau_2^0) + S_1\cos(\varphi\tau_2^0)]\cos(\varphi\tau_1) \\ & + [Q_1(\varphi)^2 - Q_3 - S_2\cos(\varphi\tau_2^0) - S_1\varphi\sin(\varphi\tau_2^0)]\sin(\varphi\tau_1) \tag{A.19} \\ & = (\varphi)^3 - P_2\varphi - R_2\varphi_1^*\cos(\varphi\tau_2^0) + (R_3 - R_1\varphi)\sin(\varphi\tau_2^0). \end{aligned}$$

Squaring and adding the two equations, and we have

$$\varphi^6 + K_{21}\varphi^4 + K_{22}\varphi^2 + K_{23} + K_{24}\sin(\varphi\tau_2^0) + K_{25}\cos(\varphi\tau_2^0) = 0, \tag{A.20}$$

where

$$\begin{aligned} K_{21} &= P_1^2 + R_1^2 - Q_1^2 - 2P_2, & K_{23} &= P_3^2 + R_3^2 - Q_3^2 - S_2^2, \\ K_{22} &= P_2^2 + R_2^2 - Q_2^2 - S_1^2 - 2P_1P_3 - 2R_1R_3 + 2Q_1Q_3, \\ K_{24} &= -2R_1\varphi^5 - 2P_1R_2\varphi^4 + 2(R_3 + P_2R_1 + Q_1S_1)\varphi^3 + 2(P_3R_2 - P_2R_3 + Q_2S_2 - Q_3S_1), \\ K_{25} &= 2(-R_2 + P_1R_2)\varphi^4 - 2(P_1R_3 + P_3R_1 - P_2R_2 + Q_2S_1 - Q_1S_2)\varphi^2 + 2P_3R_3 - 2Q_3S_2. \end{aligned}$$

Denote

$$h_2(\varphi) = \varphi^6 + K_{21}\varphi^4 + K_{22}\varphi^2 + K_{23} + K_{24}\sin(\varphi\tau_2^0) + K_{25}\cos(\varphi\tau_2^0). \tag{A.21}$$

Obviously,  $h_2(0) = K_{23} + K_{25} |_{\varphi=0} = (P_3 + R_3)^2 - (Q_3 + S_2)^2$  and  $\lim_{\varphi \rightarrow \infty} h_2(\varphi) = +\infty$ . We assume that  $h_2(0) < 0 \Rightarrow (P_3 + R_3)^2 < (Q_3 + S_2)^2$ . Then, the Eq (A.21) has at least one positive root.

Assume that Eq (A.21) has finite positive roots  $\varphi_k (k = 1, 2, \dots, l)$ . The critical value

$$\tau_{1k}^{(j)} = \frac{1}{\varphi_k} \arccos \frac{\Psi_1 \Psi_3 + \Psi_2 \Psi_4}{(\Psi_1)^2 + (\Psi_2)^2} + \frac{2\pi j}{\varphi_k}, \quad k = 1, 2, \dots, l; j = 0, 1, 2, \dots$$

where

$$\begin{aligned} \Psi_1 &= -Q_1 \varphi_k^2 + Q_3 + S_2 \cos(\varphi_k \tau_2^0) + S_1 \varphi_k \sin(\varphi_k \tau_2^0), \\ \Psi_2 &= Q_2 \varphi_k - S_2 \sin(\varphi_k \tau_2^0) + S_1 \varphi_k \cos(\varphi_k \tau_2^0), \\ \Psi_3 &= P_1 \varphi_k^2 - P_3 + (R_1 \varphi_k^2 - R_3) \cos(\varphi_k \tau_2^0) - R_2 \varphi_k \sin(\varphi_k \tau_2^0), \\ \Psi_4 &= \varphi_k^3 - P_2 \varphi_k - R_2 \varphi_k \cos(\varphi_k \tau_2^0) + (R_3 - R_1 \varphi_k^2) \sin(\varphi_k \tau_2^0). \end{aligned}$$

Let  $\hat{\tau}_{10} = \min_{k,j} \tau_{1k}^{(j)}$ ,  $k = 1, 2, \dots, l; j = 0, 1, 2, \dots$

Next, we differentiate both sides of (5.1) concerning  $\tau_1$  to verify the transversality condition.

Taking the derivative of  $\lambda$  with respect to  $\tau_1$  in (5.1) and substituting  $\lambda = i\varphi_0$ , we obtain

$$\operatorname{Re} \left( \frac{d\lambda}{d\tau_1} \right)_{\lambda=i\varphi_0}^{-1} = \frac{M_1 M_3 + M_2 M_4}{M_1^2 + M_2^2},$$

where

$$\begin{aligned} M_1 &= \varphi_0^4 - P_2 \varphi_0^2 - R_2 \varphi_0 \cos(\varphi_0 \tau_2^0) + (-R_1 \varphi_0^2 + R_3) \sin(\varphi_0 \tau_2^0), \\ M_2 &= -P_1 \varphi_0^3 + P_3 \varphi_0 + (-R_1 \varphi_0^2 + R_3) \cos(\varphi_0 \tau_2^0) + R_2 \varphi_0 \sin(\varphi_0 \tau_2^0), \\ M_3 &= 3\varphi_0^3 - P_2 - 2Q_1 \varphi_0 \sin(\varphi_0 \tau_1) - Q_2 \cos(\varphi_0 \tau_1) - 2R_1 \varphi_0 \sin(\varphi_0 \tau_2^0) \\ &\quad - R_2 \cos(\varphi_0 \tau_2^0) + (S_2 \tau_2^0 - S_1) \cos(\varphi_0(\tau_1 + \tau_2^0)) + S_1 \varphi_0 \tau_2^0 \sin(\varphi_0(\tau_1 + \tau_2^0)), \\ M_4 &= -2P_1 \varphi_0 - 2Q_1 \varphi_0 \cos(\varphi_0 \tau_1) + Q_2 \sin(\varphi_0 \tau_1) - 2R_1 \varphi_0 \cos(\varphi_0 \tau_2^0) \\ &\quad + R_2 \sin(\varphi_0 \tau_2^0) + S_1 \varphi_0 \tau_2^0 \cos(\varphi_0(\tau_1 + \tau_2^0)) + (S_1 - S_2 \tau_2^0) \sin(\varphi_0(\tau_1 + \tau_2^0)). \end{aligned}$$

If  $M_1 M_3 + M_2 M_4 > 0$  holds, then  $\operatorname{Re} \left( \frac{d\lambda}{d\tau_1} \right)_{\lambda=i\varphi_0}^{-1} > 0$ . Therefore, the transversality condition is satisfied and a Hopf-bifurcation occurs at  $E^*$  for  $\tau_1 = \hat{\tau}_{10}$ .  $\square$

### Proof of Theorem 5.8:

*Proof.* We consider that  $\tau_1 = \tau_1^0$  in its stable interval, with  $\tau_2$  as the parameter.

The calculation process is similar to Theorem 5.7.  $\square$

### References

1. A. Das, G. P. Samanta, A prey-predator model with refuge for prey and additional food for predator in a fluctuating environment, *Physica A*, **538** (2019), 427–450. <https://doi.org/10.1016/j.physa.2019.122844>

2. D. Pal, G. S. Mahaptra, G. P. Samanta, Optimal harvesting of prey-predator system with interval biological parameters: A bioeconomic model, *Math. Biosci.*, **241** (2013), 181–187. <https://doi.org/10.1016/j.mbs.2012.11.007>
3. S. Sharma, G. P. Samanta, A Leslie-Gower predator-prey model with disease in prey incorporating a prey refuge, *Chaos Soliton. Fract.*, **70** (2015), 69–84. <https://doi.org/10.1016/j.chaos.2014.11.010>
4. G. Tang, S. Tang, R. A. Cheke, Global analysis of a holling type II predator-prey model with a constant prey refuge, *Nonlinear Dynam.*, **76** (2014), 635–647. <https://doi.org/10.1007/s11071-013-1157-4>
5. J. P. Tripathi, S. Abbas, M. Thakur, A density dependent delayed predator-prey model with Beddington-DeAngelis type function response incorporating a prey refuge, *Commun. Nonlinear Sci. Numer. Simul.*, **22** (2015), 427–450. <https://doi.org/10.1016/j.cnsns.2014.08.018>
6. A. Q. Khan, S. A. H. Bukhari, M. B. Almatrafi, Global dynamics, Neimark-Sacker bifurcation and hybrid control in a Leslie's prey-predator model, *Alex. Eng. J.*, **61** (2022), 11391–11404. <https://doi.org/10.1016/j.aej.2022.04.042>
7. A. Q. Khan, F. Nazir, M. B. Almatrafi, Bifurcation analysis of a discrete Phytoplankton–Zooplankton model with linear predational response function and toxic substance distribution, *Int. J. Biomath.*, **16** (2022). <https://doi.org/10.1142/S1793524522500954>
8. A. Q. Khan, M. Tasneem, M. B. Almatrafi, Discrete-time COVID-19 epidemic model with bifurcation and control, *Alex. Eng. J.*, **19** (2022), 1944–1969. <https://doi.org/10.3934/mbe.2022092>
9. N. Mondal, H. Alrabaiah, D. Barman, J. Roy, S. Alam, Influence of predator incited fear and interference competition in the dynamics of prey-predator system where the prey species are protected in a reserved area, *Ecol. Environ. Conserv.*, **28** (2022), 831–852. <http://doi.org/10.53550/EEC.2022.v28i02.040>
10. D. Mukherjee, Role of fear in predator-prey system with intraspecific competition, *Math. Comput. Simul.*, **177** (2020), 263–275. <https://doi.org/10.1016/j.matcom.2020.04.025>
11. Y. Shao, Global stability of a delayed predator-prey system with fear and Holling-type II functional response in deterministic and stochastic environments, *Math. Comput. Simul.*, **200** (2022), 65–77. <https://doi.org/10.1016/j.matcom.2022.04.013>
12. L. Y. Zanette, A. F. White, M. C. Allen, M. Clinchy, Perceived predation risk reduces the number of offspring songbirds produce per year, *Science*, **334** (2011), 1398–1401. <https://doi.org/10.1126/science.1210908>
13. S. Creel, D. Christianson, S. Liley, J. A. Winnie, Predation risk affects reproductive physiology and demography of elk, *Science*, **315** (2007), 960. <https://doi.org/10.1126/science.1135918>
14. J. P. Suraci, M. Clinchy, L. M. Dill, D. Roberts, L. Y. Zanette, Fear of large carnivores causes a trophic cascade, *Nat. Commun.*, **7** (2016), 10698. <https://doi.org/10.1038/ncomms10698>
15. X. Wang, L. Zanette, X. Zou, Modelling the fear effect in predator-prey interactions, *J. Math. Biol.*, **73** (2016), 1179–1204. <https://doi.org/10.1007/s00285-016-0989-1>

16. C. S. Holling, The components of predation as revealed by a study of small-mammal predation of the european pine sawfly, *Canadian Entomol.*, **9** (1959), 293–320. <https://doi.org/10.4039/Ent91293-5>
17. C. S. Holling, The functional response of predators to prey density and its role in mimicry and population regulation, *Mem. Entomol. Soc. Can.*, **97** (1965), 5–60. <https://doi.org/10.4039/entm9745fv>
18. C. S. Holling, Some characteristics of simple types of predation and parasitism, *Canadian Entomol.*, **91** (1959), 385. <https://doi.org/10.4039/Ent91385-7>
19. Z. Liu, R. Yuan, Stability and bifurcation in a delayed predator-prey system with Beddington-DeAngelis functional response, *J. Math. Anal. Appl.*, **296** (2004), 521–537. <https://doi.org/10.1016/j.jmaa.2004.04.051>
20. X. Shi, X. Zhou, X. Song, Analysis of a stage-structured predator-prey model with Crowley-Martin function, *J. Appl. Math. Comput.*, **36** (2011), 459–472. <https://doi.org/10.1007/s12190-010-0413-8>
21. J. P. Tripathi, S. Tyagi, S. Abbas, Global analysis of a delayed density dependent predator-prey model with Crowley-Martin functional response, *Commun. Nonlinear Sci. Numer. Simul.*, **30** (2016), 45–69. <https://doi.org/10.1016/j.cnsns.2015.06.008>
22. R. Chinnathambi, F. A. Rihan, Stability of fractional-order prey-predator system with time-delay and monod-haldane functional response, *Nonlinear Dynam.*, **92** (2018), 1637–1648. <https://doi.org/10.1007/s11071-018-4151-z>
23. J. Roy, D. Barman, S. Alam, Role of fear in a predator-prey system with ratio-dependent functional response in deterministic and stochastic environment, *Biosystems*, **197** (2020), 104176. <https://doi.org/10.1016/j.biosystems.2020.104176>
24. M. Banerjee, Y. Takeuchi, Maturation delay for the predators can enhance stable coexistence for a class of prey-predator models, *J. Theor. Biol.*, **412** (2017), 154–171. <https://doi.org/10.1016/j.jtbi.2016.10.016>
25. B. Dubey, A. Kumar, A. P. Maiti, Global stability and Hopf-bifurcation of prey-predator system with two discrete delays including habitat complexity and prey refuge, *Commun. Nonlinear Sci. Numer. Simul.*, **67** (2019), 528–554. <https://doi.org/10.1016/j.cnsns.2018.07.019>
26. J. Zhang, Bifurcation analysis of a modified Holling-Tanner predator-prey model with time delay, *Appl. Math. Model.*, **36** (2012), 1219–1231. <https://doi.org/10.1016/j.apm.2011.07.071>
27. D. Hu, Y. Li, M. Liu, Y. Bai, Stability and Hopf bifurcation for a delayed predator-prey model with stage structure for prey and ivlev-type functional response, *Nonlinear Dynam.*, **99** (2020), 3323–3350. <https://doi.org/10.1007/s11071-020-05467-z>
28. Y. Bai, Y. Li, Stability and Hopf bifurcation for a stage-structured predator-prey model incorporating refuge for prey and additional food for predator, *Adv. Differ. Equ.*, **1** (2019), 1–20. <https://doi.org/10.1186/s13662-019-1979-6>
29. F. Chen, M. You, Permanence for an integrodifferential model of mutualism, *Appl. Math. Comput.*, **186** (2007), 30–34. <https://doi.org/10.1016/j.amc.2006.07.085>

30. E. Beretta, Y. Kuang, Geometric stability switch criteria in delay differential systems with delay-dependent parameters, *SIAM J. Math. Anal.*, **33** (2002), 1144–1165. <https://doi.org/10.1137/S0036141000376086>
31. L. Deng, X. Wang, M. Peng, Hopf bifurcation analysis for a ratio-dependent predator-prey system with two delays and stage structure for the predator, *Appl. Math. Comput.*, **231** (2014), 214–230. <https://doi.org/10.1016/j.amc.2014.01.025>
32. X. Yang, L. Chen, J. Chen, Permanence and positive periodic solution for the single-species nonautonomous delay diffusive models, *Comput. Math. Appl.*, **32** (1996), 109–116. [https://doi.org/10.1016/0898-1221\(96\)00129-0](https://doi.org/10.1016/0898-1221(96)00129-0)
33. S. L. Ross, *Differential equations*, New York: John Wiley and Sons, 1984.



AIMS Press

©2023 the Author(s), licensee AIMS Press. This is an open access article distributed under the terms of the Creative Commons Attribution License (<http://creativecommons.org/licenses/by/4.0>)